




Complete Characterization of Phase and Amplitude of Bichromatic Extreme Ultraviolet Light

Michele Di Fraia,¹ Oksana Plekan,¹ Carlo Callegari¹,, Kevin C. Prince^{1,2,*},, Luca Giannessi,^{1,3} Enrico Allaria,¹ Laura Badano,¹ Giovanni De Ninno,^{1,4} Mauro Trovò,¹ Bruno Diviacco,¹ David Gauthier,^{1,‡} Najmeh Mirian,¹ Giuseppe Penco,¹ Primož Rebernik Ribič,¹ Simone Spampinati,¹ Carlo Spezzani,¹ Giulio Gaio,¹ Yuki Orimo,⁵ Oyunbileg Tugs,⁵ Takeshi Sato,^{5,6,7} Kenichi L. Ishikawa^{5,6,7},, Paolo Antonio Carpeggiani,⁸ Tamás Csizmadia,⁹ Miklós Füle,⁹ Giuseppe Sansone,¹⁰ Praveen Kumar Maroju,¹⁰ Alessandro D'Elia,^{11,12} Tommaso Mazza,¹³ Michael Meyer,¹³ Elena V. Gryzlova,¹⁴ Alexei N. Grum-Grzhimailo,¹⁴ Daehyun You,¹⁵ and Kiyoshi Ueda^{15,†}

¹*Elettra-Sincrotrone Trieste S.C.p.A, 34149 Basovizza, Trieste, Italy*

²*Centre for Translational Atomaterials, Swinburne University of Technology, Melbourne 3122, Australia*

³*INFN—Laboratori Nazionali di Frascati, 00044 Frascati, Rome, Italy*

⁴*Laboratory of Quantum Optics, University of Nova Gorica, 5001 Nova Gorica, Slovenia*

⁵*Department of Nuclear Engineering and Management, Graduate School of Engineering, The University of Tokyo, 7-3-1 Hongo, Bunkyo-ku, Tokyo 113-8656, Japan*

⁶*Photon Science Center, Graduate School of Engineering, The University of Tokyo, 7-3-1 Hongo, Bunkyo-ku, Tokyo 113-8656, Japan*

⁷*Research Institute for Photon Science and Laser Technology, The University of Tokyo, 7-3-1 Hongo, Bunkyo-ku, Tokyo 113-0033 Japan*

⁸*Institut für Photonik, Technische Universität Wien, 1040 Vienna, Austria*

⁹*ELI-ALPS, ELI-HU Non-Profit Ltd., H-6720 Szeged, Hungary*

¹⁰*Physikalisches Institut, Albert-Ludwigs-Universität Freiburg, 79106 Freiburg, Germany*

¹¹*University of Trieste, Department of Physics, 34127 Trieste, Italy*

¹²*IOM-CNR, Laboratorio Nazionale TASC, 34149 Basovizza, Trieste, Italy*

¹³*European XFEL GmbH, D-22869 Schenefeld, Germany*

¹⁴*Skobeltsyn Institute of Nuclear Physics, Lomonosov Moscow State University, Moscow 119991, Russia*

¹⁵*Institute of Multidisciplinary Research for Advanced Materials, Tohoku University, Sendai 980-8577, Japan*



(Received 27 May 2019; published 22 November 2019)

Intense, mutually coherent beams of multiharmonic extreme ultraviolet light can now be created using seeded free-electron lasers, and the phase difference between harmonics can be tuned with attosecond accuracy. However, the absolute value of the phase is generally not determined. We present a method for determining precisely the absolute phase relationship of a fundamental wavelength and its second harmonic, as well as the amplitude ratio. Only a few easily calculated theoretical parameters are required in addition to the experimental data.

DOI: [10.1103/PhysRevLett.123.213904](https://doi.org/10.1103/PhysRevLett.123.213904)

Quantum mechanical processes, such as photoionization, are defined by the amplitudes and phases of the particles involved, and their description requires the determination of all of these, as, for example, in complete experiments [1–3]. While amplitudes can often be deduced from experimental intensities, the determination of phase is usually more challenging. Phase determination implies the concept of coherence, intrinsic in the nature of waves but not relevant for classical particles. Photoionization is one of the best showcases for such quantum mechanical concepts, as the phase of the photons is imprinted on the emitted electron wave function.

Recently, coherent optical experiments have become possible at short wavelengths using a seeded free-electron laser (FEL), so that multiharmonic extreme ultraviolet

(XUV) radiation can be used to coherently control the outcome of experiments [4,5]. The phase tuning of the light field does not involve the use of a traditional delay line but instead utilizes a technique based on accelerator physics in which the electron beam, rather than the light, is delayed to adjust the phase shift [6]. In the first group of experiments [4,5,7], the relative phase between a fundamental wavelength and its second harmonic was tuned with a precision of a few attoseconds, but the absolute phase difference was unknown, that is, the zero of the phase scale was not determined. Further experiments are planned: coherent control experiments using bichromatic light like the examples above, the production of XUV pulse trains via a finite number of coherent harmonics, and other more exotic schemes.

The key to all of these methods is control of the amplitude and phase of each harmonic component, so it is important to know both of these precisely. This knowledge is also indispensable for theoretical predictions and simulations of the experiments. The relative amplitudes of two wavelengths can be controlled (e.g., by gas and solid filters, or via accelerator parameters) and measured. The phase difference can be varied very precisely [6], but it is experimentally difficult to measure it absolutely at short wavelengths. At long (optical) wavelengths, there are standard methods available for determining the phase difference between two harmonics, for instance, by frequency doubling of the fundamental and observing interference with the second harmonic [8]. Such methods are not available at short wavelengths because of the lack of suitable nonlinear materials. Only recently has soft x-ray second-harmonic generation at a surface been demonstrated using FEL radiation [9], but this is far from a practical diagnostic.

The method we describe employs gas phase targets and can be used at a range of wavelengths. It requires the ionization of an ns electron (n is the principal quantum number), and we demonstrate the method for the He atom. For future coherent control experiments at soft x-ray FELs, it will be important to control and measure the phase at innershell excitation energies, and the method we present can be applied to this task, using other atomic subshells such as Ne $2s$, C $1s$, Ne $1s$, etc.

The reason that it is difficult to measure phase at a FEL is as follows. Free-electron laser radiation is generated by relativistic electrons passing through several arrays of magnets known as undulators. The wavelength is selected by tuning the magnetic field of each undulator to the appropriate, resonant value for which the electrons lag the radiation by exactly one period every undulator period. Between each pair of undulators, there are fringe magnetic fields, which lengthen the path of the electron beam by a quantity that is not necessarily an integral value of the radiation wavelength and causes consecutive undulators to emit out of phase. For single-wavelength operation, this path length difference is compensated by the use of phase shifters [6]; under the assumption that the output is maximal when all undulators emit in phase, a lookup table is generated for all phase shifters and all wavelengths.

Bichromatic light is created by tuning the magnetic field of one or more undulators to the resonant condition for a harmonic wavelength, and in the following we consider only the fundamental plus second-harmonic configuration, i.e., wavelengths λ and $\lambda/2$ (and the corresponding frequencies ω and 2ω). We first tried to use the single-wavelength lookup table to produce a new one for the bichromatic configuration, assuming that extra delays from undulator fringe fields are evenly distributed along the space between undulators. This method was not sufficiently precise to guarantee the accuracy required by the

experiment (as an example: 10 as corresponds to a phase of $2\pi/10$ at 30 nm).

If the absolute phases were known at a reference pair of wavelengths λ_r and $\lambda_r/2$, one could consider keeping the undulator gaps fixed and tuning to another wavelength by changing the electron beam energy in the accelerator. However, experimental tests with a 3% electron energy change (corresponding to a 6% wavelength change) showed that the necessary readjustment of the accelerator in terms of trajectory, quadrupole strength, and undulator resonance could not guarantee the desired phase stability.

Besides the insurmountable difficulties we just illustrated, these two unsuccessful methods cannot account for the phase uncertainty later introduced by the photon transport system through various optical elements (mirrors, filters, gas cell, etc). For this reason, the successful method demonstrated hereafter, which determines the absolute phase difference directly in the experimental chamber at the end of the beam line, is very appealing. It is based on nonlinear optics, and on the interference which is observed in the photoelectron angular distribution (PAD) between one- and two-photon ionization processes.

The schematic process of ionization of an ns electron is shown in Fig. 1. For two-photon ionization by linearly polarized light of frequency ω , there are two outgoing partial waves of s and d character, while for single-photon ionization by frequency 2ω , there is a single outgoing p wave. These three outgoing waves interfere to give a PAD which depends on their relative phases.

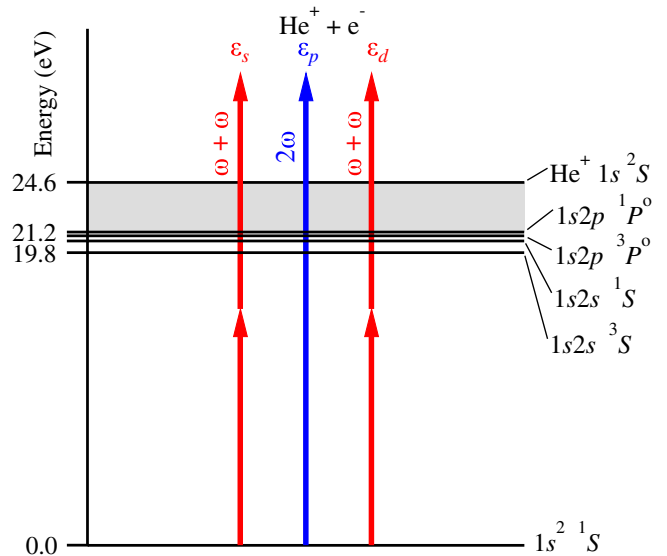


FIG. 1. Schematic process of interference between the partial photoelectron waves created by single- and two-photon ionizations. The (short) red arrows mark the fundamental photon, while the (long) blue one indicates the second harmonic. The horizontal lines show the lowest energy levels of helium.

The field is described by

$$E(t) = \sqrt{I_\omega(t)} \cos \omega t + \sqrt{I_{2\omega}(t)} \cos(2\omega t - \phi), \quad (1)$$

where $I_\omega(t)$, $I_{2\omega}(t)$ are the envelopes of the two pulses, and ϕ denotes the absolute ω - 2ω relative phase (the larger the value of ϕ , the more delayed the 2ω pulse). The experimental phase setting is $\phi' = \phi + \phi_0$, where ϕ_0 is an unknown phase offset. ϕ' is derived from a reading of the position of the magnetic structure creating the delay of the electrons [6] and can be controlled with a resolution of a few attoseconds [4]. ϕ_0 corresponds to additional delays introduced by magnetic stray fields and photon transport.

Within perturbation theory and the rotating wave approximation, and for parallel, linearly polarized long pulses, the most general form of the PAD $I_e(\theta)$ is the modulus squared of a combination of spherical harmonics $Y_{\ell,m}$ with angular momentum ℓ up to 2, and $m = 0$:

$$I_e(\theta) = |c_s e^{i\eta_s} Y_{0,0}(\theta, \varphi) + c_p e^{i(\eta_p + \phi)} Y_{1,0}(\theta, \varphi) + c_d e^{i\eta_d} Y_{2,0}(\theta, \varphi)|^2, \quad (2)$$

where c_s , c_p , and c_d are amplitudes of partial waves, θ is the polar angle with respect to the electric vector (the azimuthal angle φ is redundant), and η_s , η_p , η_d are scattering phase shifts. The volume of the interaction region is not taken into account. Equation (2) is traditionally written as a series expansion of Legendre polynomials $P_\ell(\cos \theta)$,

$$I_e(\theta) = \frac{(c_s^2 + c_p^2 + c_d^2)}{4\pi} \left(1 + \sum_{\ell=1}^4 \beta_\ell P_\ell(\cos \theta) \right), \quad (3)$$

and the expression of the asymmetry parameters β_ℓ as a function of c_s , c_p , c_d [Eqs. (4)–(7), with $h = 1$] is found, after some tedious algebra, using the identities (S1) and (S5)–(S7) in the Supplemental Material [10].

Experimentally, there are a number of challenges to be faced, due to nonideal experimental conditions, such as variations of intensity across the excitation volume, incomplete coherence, small misalignments of the focal spots, etc. We define the decoherence parameter $h \in [0, 1]$ which we use to phenomenologically correct for these imperfections, and to scale the β_1 and β_3 oscillations. The resulting expressions for β_i are

$$\beta_1 = h \times \frac{4\sqrt{15}c_d c_p \cos(-\eta_d + \eta_p + \phi) + 10\sqrt{3}c_p c_s \cos(\eta_p - \eta_s + \phi)}{5(c_d^2 + c_p^2 + c_s^2)}, \quad (4)$$

$$\beta_2 = \frac{10c_d^2 + 14\sqrt{5}c_d c_s \cos(\eta_d - \eta_s) + 14c_p^2}{7(c_d^2 + c_p^2 + c_s^2)}, \quad (5)$$

$$\beta_3 = h \times \frac{6\sqrt{15}c_d c_p \cos(-\eta_d + \eta_p + \phi)}{5(c_d^2 + c_p^2 + c_s^2)} \equiv [\beta_3]_0 \cos[\phi' - (\phi_0 + \eta_d - \eta_p)], \quad (6)$$

$$\beta_4 = \frac{18c_d^2}{7(c_d^2 + c_p^2 + c_s^2)}, \quad (7)$$

$$\beta_1 - \frac{2}{3}\beta_3 = h \times \frac{2\sqrt{3}c_p c_s \cos(\eta_p - \eta_s + \phi)}{c_d^2 + c_p^2 + c_s^2} \equiv \left[\beta_1 - \frac{2}{3}\beta_3 \right]_0 \cos[\phi' - (\phi_0 - \eta_p + \eta_s)]. \quad (8)$$

Equation (8) is derived from Eqs. (4) and (6) so that, like Eq. (6), the right-hand side can be factored into a cosine containing the optical and scattering phase dependence, and an amplitude independent of phase (the prefactor in square brackets). We note that Eqs. (5) and (7) for β_ℓ , where ℓ is even, do not depend on phase, in agreement with previous results [13,14].

Equations (6) and (8) are among the main results of this Letter. At fixed photon energy, a graph of these quantities against experimental phase ϕ' yields two oscillatory curves

whose absolute phases are independent of photon intensity. For the particular case of He, the values of scattering phase shifts η_s , η_p , and η_d for a wide range of electron energies are available in the literature [15–17]. We now show that we are able to extract two independent values of the phase offset ϕ_0 , whose excellent agreement attests to the robustness of the method. As well, further information can be extracted to benchmark the method; for example, the difference $\eta_d - \eta_s$ can be determined from the phase difference of the curves of Eqs. (8) and (6).

The amplitude of the oscillatory curves depends on the coherent mixing of the two photon fields: the ratio c_s/c_d can also be extracted from Eqs. (8) and (6). The ratio of the two amplitudes of oscillation, $[\beta_1 - \frac{2}{3}\beta_3]_0$ and $[\beta_3]_0$, is equal to c_s/c_d multiplied by the numerical factor $\sqrt{5}/3$. Further manipulation of all equations yields the ratio $(c_s^2 + c_d^2)/c_p^2$, which in combination with theoretical calculations yields the relative intensities of the two fields. At fixed photon energy, a graph of these quantities against phase yields two oscillatory curves. Their relative phase is determined by the argument of the cosine functions and is independent of photon intensity. The amplitude of the oscillatory curves is independent of phase, but does depend on the amplitude of the photon field. From the relative amplitudes of the curves, we may extract information about the effective relative photon amplitudes, even in the case of imperfect experimental conditions.

The photoionization processes can be accurately simulated using the time-dependent close-coupling (TDCC) method [18,19] or the multiconfiguration time-dependent Hartree-Fock (MCTDHF) method [20–25]. We have performed TDCC simulations for a series of photon energies and list the values of c_s , c_p , and c_d relevant for this experiment in Table I. In Table II of the Supplemental Material [10], we compare the values of $\eta_s - \eta_d$ and $\eta_p - \eta_d$ from our simulations with those reported in Ref. [17], and they agree very well. We have also confirmed that the PADs obtained from TDCC and MCTDHF simulations are in excellent agreement with each other. In the present TDCC calculations, the amplitudes are normalized so that $c_s^2 + c_d^2$ and c_p^2 correspond to the degree of ionization by ω and 2ω , respectively, for a 7 fs pulse duration. This value is much shorter than the experimental duration and was chosen for reasons of computational economy. So long as the bandwidth of the pulse is sufficiently far from any atomic resonance, one can safely scale the results to the present longer experimental pulses [18,19]. Note that, for a given photon energy, $\hbar\omega$, c_s^2 , c_p^2 , and c_d^2 scale linearly with pulse duration; c_s and c_d scale as I_ω , whereas c_p scales as $\sqrt{I_{2\omega}}$. Thus, one can calculate β parameters for any intensity and pulse duration from these tabulated values as long as the

perturbative treatment is valid, and processes of higher order than those considered here are negligible.

We used a velocity map imaging (VMI) spectrometer [26] to measure the PAD described by Eq. (3) (alternative instruments include multidetector electron time-of-flight spectrometers [27,28]). The angular distributions and photoelectron spectra were determined by analysis after inversion of the velocity map images. The sample was irradiated with fundamental radiation at one of the wavelengths $\lambda = 87.0$, 78.0, or 65.0 nm, and its second harmonic $\lambda/2 = 43.5$, 39.0, 32.5 nm, and the PAD was measured. The second-harmonic intensity was set so that the measured ratios of ionization rates due to single- and two-photon ionization were close to 2:1 for datasets A, B, and C, while for dataset D, it was 4:1. The phase was tuned using the phase shifters installed at FERMI [6]. The intensities were sufficient to cause significant ionization, without danger of saturation effects; see Supplemental Material [10].

From the VMI data, we extracted β_1 , β_2 , β_3 , and β_4 as a function of the experimental relative phase $\phi' = \phi + \phi_0$ between the two optical pulses of ω and 2ω [see Eq. (1)]. An example of the results for dataset A at 14.3 eV is shown in Fig. 2, where β_2 , β_3 , β_4 , and $\beta_1 - \frac{2}{3}\beta_3$ are shown. As expected, β_3 and $\beta_1 - \frac{2}{3}\beta_3$ oscillate while β_2 and β_4 are constant. From least-squares fitting of the data with cosine curves and offsets, we extracted six parameters, β_2 , β_4 , $[\beta_3]_0$, $\phi_0 + \eta_d - \eta_p$, $[\beta_1 - \frac{2}{3}\beta_3]_0$, and $\phi_0 - \eta_p + \eta_s$. The results are given in Table II for four datasets that we recorded.

To determine ϕ_0 from the measurements, we substituted the calculated values of phase (see Table II of the Supplemental Material [10]) into Eqs. (6) and (8) and obtained two values of the phase offset ϕ_0 (see Table II), which agree to within 0.03–0.04 rad, or 2 deg. Figure 2 illustrates this, where it can be seen that the choice of η_p and either η_s or η_d yields the values of ϕ_0 and of the remaining η .

There is a large difference in the values of ϕ_0 for different datasets, for example B and C: this is because the two sets were taken about 68 h apart, after numerous changes of undulator magnetic fields, and small corrections to the

TABLE I. *Ab initio* results using the TDCC method. Both ω and 2ω pulses are assumed to have a Gaussian temporal profile with 7 fs FWHM pulse duration. The peak intensity of ω is fixed at 10^{13} W/cm². $I_{2\omega}^{\max}$ is the 2ω peak intensity at which the ionization yields by ω and 2ω pulses ($c_s^2 + c_d^2$ and c_p^2 , respectively) are equal to each other. The values of c_s , c_p , and c_d are listed for this condition. $\sigma_\omega^{(2)}$ is the cross section for two-photon ionization by the ω pulse, $\sigma_{2\omega}^{(1)}$ is the cross section for single-photon ionization by the 2ω pulse.

$\hbar\omega$ (eV)	$I_{2\omega}^{\max}$ (W/cm ²)	c_s	c_p	c_d	$\eta_s - \eta_d$ (rad)	$\eta_p - \eta_d$ (rad)	$\sigma_\omega^{(2)}$ (10 ⁻⁵² cm ⁴ /s)	$\sigma_{2\omega}^{(1)}$ (10 ⁻¹⁸ cm ²)
14.3	1.34×10^{10}	3.22×10^{-3}	1.14×10^{-2}	-1.09×10^{-2}	5.36	2.26	12.9	5.92
15.9	1.24×10^{10}	1.77×10^{-3}	9.44×10^{-3}	-9.28×10^{-3}	5.07	2.12	11.0	4.92
19.1	1.09×10^{10}	-4.76×10^{-4}	6.81×10^{-4}	-6.79×10^{-4}	4.76	1.985	8.24	3.44

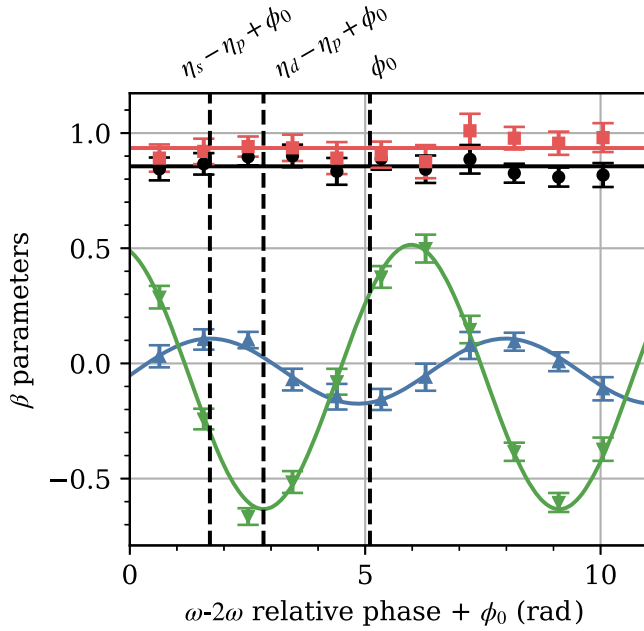


FIG. 2. β parameters as a function of ϕ . Markers, β parameters of dataset A as a function of phase; curves, cosine (constant) fit, odd (even) β ; blue triangles, $\beta_1 - 2\beta_3/3$; black circles, β_2 ; green inverted triangles, β_3 ; red squares, β_4 . Error bars show standard errors of least-squares fitting using the model described in Eq. (3). Linearly polarized light, $\lambda = 86.7$ nm, $\lambda/2 = 43.4$ nm.

accelerator trajectory. During a scan, which lasted on the order of 2 h, no changes to the accelerator were made, other than a scanning of the phase. We checked that the conditions were sufficiently stable by repeating the first points of a scan at the end of the scan, and by scanning with increasing phase, followed by decreasing phase.

Let us now return to the quantities c_s/c_d and $\eta_s - \eta_d$ extracted from the fit parameters as explained above. These quantities do not depend on the pulse intensity and thus can be directly compared with the *ab initio* results in Table I. The results for c_s/c_d and $\eta_s - \eta_d$ obtained using Eqs. (6) and (8) are also given in Table II. These two parameters agree well with theoretical values, confirming that the present methodology works well.

Let us finally consider the other two parameters, $c_p^2/(c_s^2 + c_d^2)$, which is proportional to $I_{2\omega}/I_\omega^2$, and h , which scales the amplitudes of β_1 and β_3 . To extract $c_p^2/(c_s^2 + c_d^2)$ and h from our experimental results, we optimize those parameters by minimizing χ^2 given by

$$\chi^2 = \frac{([\beta_1^{\text{exp}} - \frac{2}{3}\beta_3^{\text{exp}}]_0 - [\beta_1^{\text{th}} - \frac{2}{3}\beta_3^{\text{th}}]_0)^2}{\alpha_1^2} + \frac{(\beta_2^{\text{exp}} - \beta_2^{\text{th}})^2}{\alpha_2^2} + \frac{([\beta_3^{\text{exp}}]_0 - [\beta_3^{\text{th}}]_0)^2}{\alpha_3^2} + \frac{(\beta_4^{\text{exp}} - \beta_4^{\text{th}})^2}{\alpha_4^2}, \quad (9)$$

where $[\beta_1^{\text{exp}} - 2/3\beta_3^{\text{exp}}]_0$, $[\beta_3^{\text{exp}}]_0$, and $\beta_{2,4}^{\text{exp}}$ are the present experimental values, and $\alpha_1, \alpha_3, \alpha_{2,4}$ are their respective uncertainties (Table II), and the β^{th} are values calculated from Eqs. (4)–(8) with theoretical values in Table I, regarding c_p/c_d and h as fitting parameters. The resulting values are also given in Table II. As noted above, $c_p^2/(c_s^2 + c_d^2)$ is proportional to $I_{2\omega}/I_\omega^2$, so we can determine $\sqrt{I_{2\omega}/I_\omega}$, as given in Table II, by employing the theoretical ratio of $c_p^2/(c_s^2 + c_d^2)$ in Table I.

In conclusion, we have demonstrated a method of determining the absolute phase between two wavelengths in a bichromatic XUV beam, as well as the coherent fraction of the relative intensity. The determination of phase is independent of the intensity of the two wavelengths. This

TABLE II. Results of analysis of four experimental datasets at three different photon energies.

	Dataset A	Dataset B	Dataset C	Dataset D
Photon energy (eV)	14.3	15.9	15.9	19.1
$[\beta_1 - \frac{2}{3}\beta_3]_0$	0.141 ± 0.008	0.114 ± 0.008	0.057 ± 0.004	-0.030 ± 0.003
$\phi_0 - \eta_p + \eta_s$ (rad)	1.70 ± 0.05	1.75 ± 0.06	6.28 ± 0.07	1.20 ± 0.11
β_2	0.856 ± 0.010	1.631 ± 0.009	1.691 ± 0.005	1.784 ± 0.005
$[\beta_3]_0$	-0.574 ± 0.013	-0.810 ± 0.025	-0.439 ± 0.017	-0.723 ± 0.008
$\phi_0 + \eta_d - \eta_p$ (rad)	2.84 ± 0.02	3.17 ± 0.03	1.28 ± 0.04	2.28 ± 0.01
β_4	0.935 ± 0.013	1.028 ± 0.028	0.412 ± 0.009	1.010 ± 0.016
c_s/c_d (expt.)	-0.330 ± 0.021	-0.189 ± 0.014	-0.174 ± 0.013	0.055 ± 0.006
c_s/c_d (theory)	-0.295	-0.191	-0.191	0.070
$\eta_s - \eta_d$ (expt.) (rad)	5.15 ± 0.06	4.87 ± 0.07	5.01 ± 0.08	5.21 ± 0.11
$\eta_s - \eta_d$ (theory) (rad)	5.36	5.07	5.07	4.76
$c_p^2 : c_s^2 + c_d^2$	$0.82 \pm 0.01 : 1$	$1.44 \pm 0.05 : 1$	$3.58 \pm 0.06 : 1$	$1.55 \pm 0.03 : 1$
h	0.262 ± 0.006	0.360 ± 0.010	0.226 ± 0.008	0.318 ± 0.004
$\sqrt{I_{2\omega}/I_\omega}$ ($10^{-9}/\sqrt{\text{W}/\text{cm}^2}$)	10.5 ± 0.1	13.4 ± 0.2	21.1 ± 0.2	13.0 ± 0.1
ϕ_0 (rad)	5.07 ± 0.02	5.25 ± 0.03	3.38 ± 0.04	4.26 ± 0.01

is useful for several purposes: experiments at a fixed pair of wavelengths may require knowledge of the absolute phase relationship between the two in order to interpret the data, and this can be provided by adding He gas to the target. If multiple, phase locked wavelengths are used, the absolute phase can be extracted. Lastly, precise knowledge of the absolute phase difference and intensity ratio provides a far more rigorous basis for benchmarking theoretical simulations of experimental data. An advantage of the method is that it is applied at the experimental station, rather than at the exit of the FEL, so any alterations in phase difference introduced by beam transport are automatically included in the measurement.

This work was supported in part by the X-ray Free Electron Laser Utilization Research Project and the X-ray Free Electron Laser Priority Strategy Program of the Ministry of Education, Culture, Sports, Science, and Technology of Japan (MEXT) and the IMRAM program of Tohoku University, and the Dynamic Alliance for Open Innovation Bridging Human, Environment and Materials program. K. L. I. gratefully acknowledges support by the Cooperative Research Program of the Network Joint Research Center for Materials and Devices (Japan), the Grant-in-Aid for Scientific Research (Grants No. 16H03881, No. 17K05070, No. 18H03891, and No. 19H00869) from MEXT, JST COI (Grant No. JPMJCE1313), JST CREST (Grant No. JPMJCR15N1), and the Japan-Hungary Research Cooperative Program, JSPS and HAS. E. V. G. acknowledges the Foundation for the Advancement of Theoretical Physics and Mathematics “BASIS.” D. Y. acknowledges supports from JSPS KAKENHI Grant No. JP19J12870, and a Grant-in-Aid of Tohoku University Institute for Interdisciplinary Advanced Research and Education. T. M and M. M. acknowledge support by Deutsche Forschungsgemeinschaft Grant No. SFB925/A1. We acknowledge the support of the Alexander von Humboldt Foundation (Project Tirinto), the Italian Ministry of Research Project FIRB No. RBID08CRXX and No. PRIN 2010 ERFKXL 006, the bilateral project CNR JSPS Ultrafast science with extreme ultraviolet Free Electron Lasers, and funding from the European Union Horizon 2020 research and innovation program under the Marie Skłodowska-Curie Grant Agreement No. 641789 MEDEA (Molecular ElectronDynamics investigated by Intense Fields and Attosecond Pulses). We thank the machine physicists of FERMI for making this experiment possible with their excellent work in providing high quality FEL light.

*prince@elettra.eu

†kiyoshi.ueda@tohoku.ac.jp

‡Present address: LIDYL, CEA, CNRS, Université Paris-Saclay, CEA-Saclay, 91191 Gif-sur-Yvette, France.

- [1] U. Becker and B. Langer, *Phys. Scr.* **T78**, 13 (1998).
- [2] H. Kleinpoppen, B. Lohmann, and A. N. Grum-Grzhimailo, *Perfect/Complete Scattering Experiments* (Springer, Berlin, 2013).
- [3] P. Carpeggiani, E. V. Gryzlova, M. Reduzzi, A. Dubrouil, D. Faccialà, M. Negro, K. Ueda, S. M. Burkov, F. Frassetto, F. Stienkemeier, Y. Ovcharenko, M. Meyer, O. Plekan, P. Finetti, K. C. Prince, C. Callegari, A. N. Grum-Grzhimailo, and G. Sansone, *Nat. Phys.* **15**, 170 (2019).
- [4] K. C. Prince *et al.*, *Nat. Photonics* **10**, 176 (2016).
- [5] L. Giannessi, E. Allaria, K. C. Prince, C. Callegari, G. Sansone, K. Ueda, T. Morishita, C. N. Liu, A. N. Grum-Grzhimailo, E. V. Gryzlova, N. Douguet, and K. Bartschat, *Sci. Rep.* **8**, 7774 (2018).
- [6] B. Diviacco, R. Bracco, D. Millo, and M. M. Musardo, in *Proceedings of the 2nd International Conference on Particle Accelerators (IPAC 2011), San Sebastián, Spain, 2011*, edited by C. Petit-Jean-Genaz (IPAC'11 EPS-AG, Geneva, Switzerland, 2011), p. 3278, <http://accelconf.web.cern.ch/AccelConf/IPAC2011/index.htm>.
- [7] D. Iablonskyi *et al.*, *Phys. Rev. Lett.* **119**, 073203 (2017).
- [8] Z.-M. Wang and D. S. Elliott, *Phys. Rev. Lett.* **87**, 173001 (2001).
- [9] R. K. Lam, S. L. Raj, T. A. Pascal, C. D. Pemmaraju, L. Foglia, A. Simoncig, N. Fabris, P. Miotti, C. J. Hull, A. M. Rizzuto *et al.*, *Phys. Rev. Lett.* **120**, 023901 (2018).
- [10] See Supplemental Material at <http://link.aps.org/supplemental/10.1103/PhysRevLett.123.213904>, which includes Refs. [11,12], for further experimental details, results of calculations, and data samples.
- [11] F. W. J. Olver, A. B. O. Daalhuis, D. W. Lozier, B. I. Schneider, R. F. Boisvert, C. W. Clark, B. R. Miller, and B. V. Saunders, NIST Digital Library of Mathematical Functions, release 1.0.23, <http://dlmf.nist.gov/> (retrieved June 2019).
- [12] J. C. Adams, *Proc. R. Soc. London* **27**, 63 (1878).
- [13] A. N. Grum-Grzhimailo, E. V. Gryzlova, E. I. Staroselskaya, J. Venzke, and K. Bartschat, *Phys. Rev. A* **91**, 063418 (2015).
- [14] L. Giannessi, E. Allaria, K. C. Prince, C. Callegari, G. Sansone, K. Ueda, T. Morishita, C. N. Liu, A. N. Grum-Grzhimailo, E. V. Gryzlova, N. Douguet, and K. Bartschat, *Sci. Rep.* **8**, 7774 (2018).
- [15] D. H. Oza, *Phys. Rev. A* **33**, 824 (1986).
- [16] T. N. Chang and T. K. Fang, *Phys. Rev. A* **52**, 2638 (1995).
- [17] T. N. Gien, *J. Phys. B* **35**, 4475 (2002).
- [18] K. L. Ishikawa and K. Ueda, *Phys. Rev. Lett.* **108**, 033003 (2012).
- [19] K. L. Ishikawa and K. Ueda, *Appl. Sci.* **3**, 189 (2013).
- [20] J. Zanghellini, M. Kitzler, C. Fabian, T. Brabec, and A. Scrinzi, *Laser Phys.* **13**, 1064 (2003).
- [21] T. Kato and H. Kono, *Chem. Phys. Lett.* **392**, 533 (2004).
- [22] J. Caillat, J. Zanghellini, M. Kitzler, O. Koch, W. Kreuzer, and A. Scrinzi, *Phys. Rev. A* **71**, 012712 (2005).
- [23] T. Sato and K. L. Ishikawa, *Phys. Rev. A* **88**, 023402 (2013).

- [24] T. Sato, K.L. Ishikawa, I. Březinová, F. Lackner, S. Nagele, and J. Burgdörfer, *Phys. Rev. A* **94**, 023405 (2016).
- [25] Y. Orimo, T. Sato, A. Scrinzi, and K.L. Ishikawa, *Phys. Rev. A* **97**, 023423 (2018).
- [26] V. Lyamayev *et al.*, *J. Phys. B* **46**, 164007 (2013).
- [27] M. Ilchen, L. Glaser, F. Scholz, P. Walter, S. Deinert, A. Rothkirch, J. Seltmann, J. Viefhaus, P. Decleva *et al.*, *Phys. Rev. Lett.* **112**, 023001 (2014).
- [28] E. Allaria, B. Diviacco, C. Callegari, P. Finetti, B. Mahieu, J. Viefhaus, M. Zangrando, G. De Ninno, G. Lambert *et al.*, *Phys. Rev. X* **4**, 041040 (2014).